Available online at www.sciencedirect.com
ScienceDirect
Journal of Hazardous Materials 147 (2007) 297–306
Journal of Hazardous Materials
www.elsevier.com/locate/jhazmat

The adsorption of basic dye (Astrazon Blue FGRL) from aqueous solutions onto sepiolite, fly ash and apricot shell activated carbon: Kinetic and equilibrium studies

B. Karagozoglu [a], M. Tasdemir [a], E. Demirbas [b,*], M. Kobya [c]

[a] *Cumhuriyet University, Department of Environmental Engineering, 58140 Sivas, Turkey*
[b] *Gebze Institute of Technology, Department of Chemistry, 41400 Gebze, Turkey*
[c] *Gebze Institute of Technology, Department of Environmental Engineering, 41400 Gebze, Turkey*

Received 2 May 2006; received in revised form 22 December 2006; accepted 2 January 2007
Available online 7 January 2007

Abstract

In this study, sepiolite, fly ash and apricot stone activated carbon (ASAC) were used as adsorbents for the investigation of the adsorption kinetics, isotherms and thermodynamic parameters of the basic dye (Astrazon Blue FGRL) from aqueous solutions at various concentrations (100–300 mg/L), adsorbent doses (3–12 g/L) and temperatures (303–323 K). The result showed that the adsorption capacity of the dye increased with increasing initial dye concentration, adsorbent dose and temperature. Three kinetic models, the pseudo-first-order, second-order, intraparticle diffusion, were used to predict the adsorption rate constants. The kinetics of adsorption of the basic dye followed pseudo-second-order kinetics. Equations were developed using the pseudo-second-order model which predicts the amount of the basic dye adsorbed at any contact time, initial dye concentration and adsorbent dose within the given range accurately. The adsorption equilibrium data obeyed Langmuir isotherm. The adsorption capacities (Q_0) calculated from the Langmuir isotherm were 181.5 mg/g for ASAC, 155.5 mg/g for sepiolite and 128.2 mg/g for fly ash at 303 K. Thermodynamical parameters were also evaluated for the dye–adsorbent systems and revealed that the adsorption process was endothermic in nature.

Keywords: Adsorption kinetics; Pseudo-first-order kinetics; Pseudo-second-order kinetics; Intraparticle diffusion; Adsorption isotherms; Thermodynamic parameters

1. Introduction

Cationic dyes known as basic dyes are widely used in acrylic, nylon, silk, and wool dyeing. A large volume of dye-contaminated effluent is discharged in textile dyeing processes, and 10–15% of the dye is lost in the dye effluent. The colored wastewater damages the aesthetic nature of water and reduces the light penetration through the water's surface and the photosynthetic activity of aquatic organisms due to the presence of metals, chlorides, etc., in them [1]. Basic dyes can also cause allergic dermatitis, skin irritation, cancer, and mutations. Therefore, it is necessary to remove the dye pollutions. There are several methods for dye removals, such as coagulation and chemical oxidation, membrane separation process, electrochemical, filtration, reverse osmosis and aerobic and anaerobic microbial degradation but all of these methods suffer from one or other limitations, and none of them were successful in completely removing the color from wastewater. Dyes can be effectively removed by adsorption process; in which dissolved dye compounds attach themselves to the surface of adsorbents. Granular or powdered activated carbon is the most widely used adsorbent for the removal of colors and treatment of textile effluents because it has an excellent high surface area and high adsorption capacity for organic compounds, but its use is usually limited due to its high cost [2–4].

For this reason, many researchers have investigated for cheaper and efficient alternative substitutes to remove dyes from wastewater such as various activated carbons [5–9], agricultural wastes [10,11], sepiolite [12–14] and fly ash [15–17]. Natural adsorbents in studies involving the removal of basic dyes from aqueous solutions [18–20] are reported in the literature.

* Corresponding author. Tel.: +90 262 6053108; fax: +90 262 6053101.
E-mail address: erhan@gyte.edu.tr (E. Demirbas).

0304-3894/$ – see front matter © 2007 Elsevier B.V. All rights reserved.
doi:10.1016/j.jhazmat.2007.01.003

In the present study, the adsorption abilities of apricot stone activated carbon (ASAC), fly ash and sepiolite as adsorbents for removal of the basic dye from synthetic aqueous solutions were examined. Effects of initial dye concentration, adsorbent dose and temperature on these adsorbents under kinetic and equilibrium conditions were investigated. The rate limiting step of the dye onto the adsorbents is determined from the adsorption kinetic results. Both Langmuir and Freundlich adsorption isotherms were applied to the experimental results and thermodynamic parameters were also calculated.

2. Materials and methods

2.1. Materials

Three adsorbents were used for removal of the basic dye from the aqueous solutions which are fly ash, sepiolite and ASAC. The fly ash was obtained from Afsin-Elbistan Thermal Power Station in Turkey. The Afsin-Elbistan power plant consumes 18×10^6 metric tonnes of coal per year and generates about 3.24×10^6 metric tonnes of fly ash returning to the dumping area of the mine as combustion waste. The chemical composition of used fly ash as oxides in wt.% was SiO_2 15.14, Al_2O_3 7.54, Fe_2O_3 3.30, CaO 23.66, MgO 4.50, K_2O 0.28, Na_2O 0.57, TiO_2 1.03, SO_3 13.22. Specific surface area, bulk density, specific gravity and LOI of the fly ash have been determined as 0.342 m^2/g, 1.05 g/cm^3, 2.70 g/cm^3 and 2.31 wt.%, respectively. The particle size distribution of the fly ash was found between 2 and 300 μm [15].

Sepiolite samples used in this work were obtained from Eskisehir, Turkey. Sepiolite is a natural hydrated magnesium silicate clay mineral, $(Si_{12})(Mg_8)O_{30}(OH)_6(OH_2)_4 \cdot 8H_2O$. Structurally it is formed by blocks and channels extending in the fiber direction. Sepiolite has several adsorption applications due to its channel structure [14]. The surface area, cation exchange capacity, density and particle sizes of sepiolite are 234.3 m^2/g, 299 mmol/kg, 2.5 g/mL and 0.30–1.60 mm, respectively [12,21].

Apricot stones were obtained from Malatya in Turkey. Chemical activation were carried out by using H_2SO_4 at moderate temperatures produces a high surface area and high degree of microporosity. The parameters of ASAC are bulk density 0.43 g/mL, ash content 2.21%, pH 6.0, moisture content 7.18%, surface area 566 m^2/g, solubility in water 0.85%, solubility in 0.25 M HCl 1.22%, decolorising power 22.8 mg/g, iodine number 548 mg/g and particle size 1.00–1.25 mm, respectively [6,22]. Astrazon Blue FGRL obtained from Dystar was used for the adsorption study. This dye consists of two main components which are C.I. Basic Blue 159 and C.I. Basic Blue 3. The ratio of the two components is 5:1 (w/w), respectively. The structures of these two dye components are displayed in Fig. 1. The basic dye is not regarded as acutely toxic, but it can have various harmful effects [9]. On inhalation, it can give rise to short periods of rapid or difficult breathing. This dye is mainly used as acrylic dyeing in the industry.

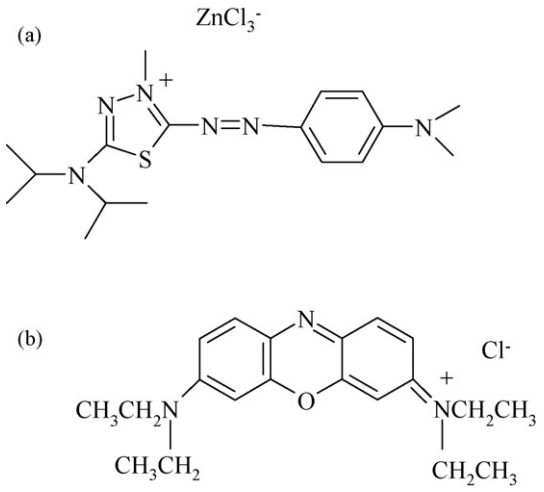

Fig. 1. Chemical structures of (a) C.I. Basic Blue 159 and (b) C:I. Basic Blue 3.

2.2. Methods

The effects of important parameters such as, initial dye concentration, adsorbent dose and temperature on the adsorptive removal of the basic dye were investigated by batch experiments. In each kinetic experiment, a known quantity of adsorbent contacted with a dye solution in a 100 mL flask at desired pH and temperature was shaken in a thermostat rotary shaker at constant agitation speed (250 rpm) for a given time intervals. At various time intervals, the flasks were successively removed, the liquid was separated from the solid by centrifugation, and the remaining concentration of dye in solution was measured spectrophotometrically on a Perkin-Elmer UV–vis spectrophotometer model 550S at a wavelength of 576 nm. In the adsorption isotherm experiments, dye solutions were added to different quantities of adsorbents into flasks and subsequently placed on a shaker for 24 h.

The concentration retained in the adsorbent phase (q_e, mg/g) was calculated by using the following equation:

$$q_e = \frac{(C_0 - C_t)V}{W_s} \quad (1)$$

where C_0 is the initial dye concentration, C_t the dye concentration (mg/L) at any time (t), V the volume of solution (L) and W_s is the mass of the adsorbent (g). Each experiment was carried out in duplicate and the average deviation between experimental and predicted one lies between ±5%.

3. Adsorption kinetics

The study of adsorption kinetics describes the solute uptake rate and evidently this rate controls the residence time of adsorbate uptake at the solid–solution interface. Adsorption rate constants for the basic dye were calculated by using pseudo-first-order, second-order and intraparticle diffusion kinetic models [23,24] which were used to describe the mechanism of the dye adsorption. The conformity between the experimental data and the model-predicted values was expressed by the correlation coefficients (r^2). A relatively high r^2 value indicates

that the model successfully describes the kinetics of the dye adsorption.

3.1. The pseudo-first-order equation

A pseudo-first-order equation can be expressed in a linear form as

$$\log(q_e - q) = \log(q_e) - \frac{k_1}{2.303}t \quad (2)$$

where q_e and q are the amount of dye adsorbed (mg/g) on the adsorbents at the equilibrium and at time t, respectively, and k_1 is the rate constant of adsorption (min^{-1}). Values of k_1 were calculated from the plots of $\log(q_e - q)$ versus t for different concentrations of the basic dye.

3.2. The pseudo-second-order equation

The pseudo-second-order adsorption kinetic rate equation is expressed as

$$\frac{dq_t}{dt} = k_2(q_e - q_t)^2 \quad (3)$$

where k_2 is the rate constant of pseudo-second-order adsorption (g/mg min). Integrating and applying the initial conditions, we have a linear form as

$$\left(\frac{t}{q_t}\right) = \frac{1}{k_2 q_e^2} + \frac{1}{q_e}(t) \quad (4)$$

where q_e is the amount of dye adsorbed at equilibrium (mg/g). The second-order rate constants were used to calculate the initial sorption rate, $h = k_2 q_e^2$. Values of k_2 and q_e were calculated from intercept and the slope of the linear plots of t/q_t versus t.

3.3. Intraparticle diffusion

The rate constant for intraparticle diffusion (k_{id}) is calculated by the following equation:

$$q = k_{id} t^{1/2} \quad (5)$$

where q is the amount dye adsorbed (mg/g) at time (t) and k_{id} (mg/g $min^{1/2}$) is the rate constant for intraparticle diffusion. Values of k_{id} were calculated from the slope of the linear plots of q versus $t^{1/2}$.

4. Results and discussion

4.1. Effect of initial dye concentration on adsorption kinetics

The effects of initial basic dye concentrations on the rate of adsorption by sepiolite, fly ash and ASAC are explored in the range from 100 to 300 mg/L (Fig. 2). It is evident from the figure that the amount dye adsorbed increases from 16.7 to 44.5 mg/g for sepiolite, from 14.9 to 40.3 mg/g for fly ash and from 16.2 to 50.1 mg/g for ASAC, respectively. It is obvious that the removals of the dye by various adsorbents were dependent on the concentration of the dye since the increase in the initial dye concentration increased the amount of the dye adsorbed on the adsorbents. Moreover, the initial rate of adsorption was greater for higher initial dye concentration because the resistance to the dye uptake decreased as the mass transfer driving force increased.

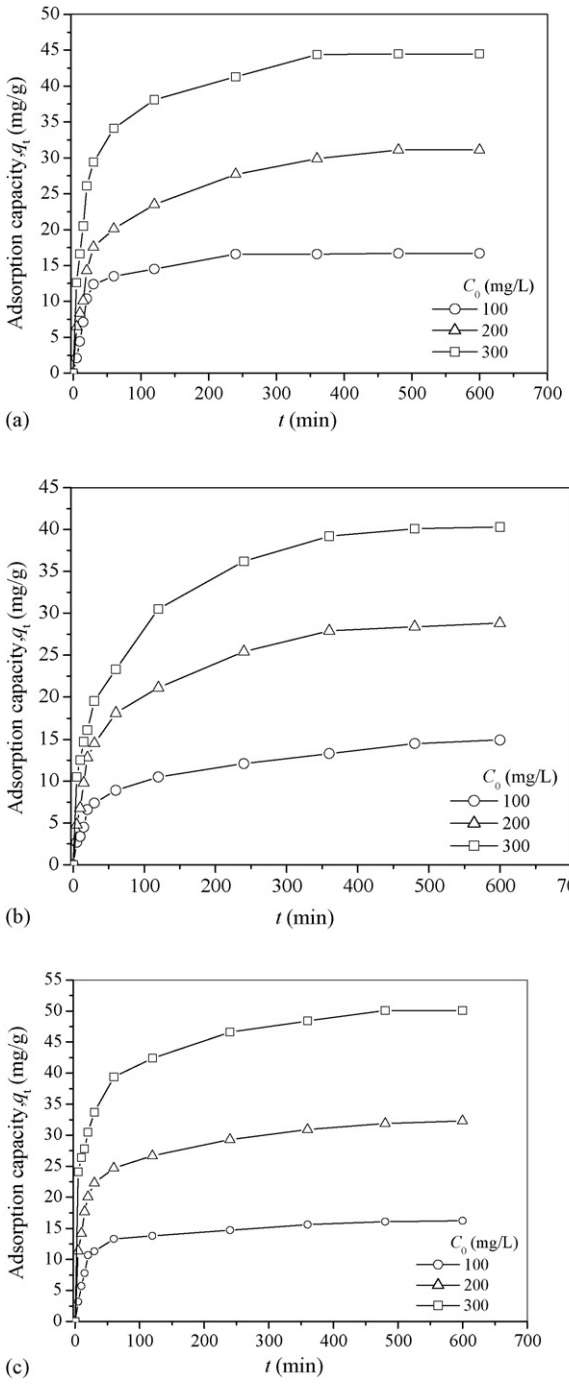

Fig. 2. The effect of initial dye concentration onto (a) sepiolite, (b) fly ash and (c) ASAC. Experimental conditions: $T = 303$ K; 250 rpm; 6 g/L.

Eqs. (2)–(5) were applied to the experimental data for the adsorption of the basic dye onto three adsorbents. The values of rate constants obtained from three kinetic models, r^2 and the predicted and experimental q_e values for the basic dye–adsorbent

Table 1
The effect of process variables on pseudo-first order model constants

Parameters	Sepiolite				Fly ash				ASAC			
	k_1 ($\times 10^2$)	$q_{e(mod)}$	$q_{e(exp)}$	r^2	k_1 ($\times 10^2$)	$q_{e(mod)}$	$q_{e(exp)}$	r^2	k_1 ($\times 10^2$)	$q_{e(mod)}$	$q_{e(exp)}$	r^2
C_0 (mg/L)												
100	1.47	10.06	16.70	0.96	0.62	10.64	14.90	0.97	0.85	8.40	16.20	0.96
200	0.80	21.24	31.10	0.97	0.83	21.01	28.80	0.98	0.74	15.70	32.30	0.97
300	1.39	29.95	44.50	0.96	0.99	31.24	40.30	0.98	0.99	25.98	50.10	0.96
m_s (g/L)												
3	0.95	27.05	65.10	0.97	0.88	24.72	55.10	0.97	0.96	33.75	57.30	0.98
6	0.80	21.24	31.10	0.97	0.83	21.01	28.80	0.98	0.74	15.70	32.30	0.97
12	1.03	11.37	16.50	0.97	0.60	8.99	14.80	0.96	0.84	6.87	16.40	0.95

Table 2
The effect of process variables on pseudo-second-order model constants

Parameters	Sepiolite					Fly ash					ASAC				
	k_2 ($\times 10^3$)	h	$q_{e(mod)}$	$q_{e(exp)}$	r^2	k_2 ($\times 10^3$)	h	$q_{e(mod)}$	$Q_{e(exp)}$	r^2	k_2 ($\times 10^3$)	h	$q_{e(mod)}$	$q_{e(exp)}$	r^2
C_0 (mg/L)															
100	3.15	0.94	17.32	16.70	0.99	1.98	0.46	15.22	14.90	0.99	3.86	1.05	16.46	16.20	0.99
200	2.19	1.72	32.24	31.10	0.99	1.11	0.99	29.99	28.80	0.99	2.17	2.30	32.56	32.30	0.99
300	1.49	3.10	45.56	44.50	0.99	0.85	1.50	41.95	40.30	0.99	1.56	4.04	50.79	50.10	0.99
m_s (g/L)															
3	0.77	6.78	65.79	65.10	0.99	0.66	4.86	55.77	55.10	0.99	1.00	3.47	58.69	57.30	0.99
6	1.16	1.72	32.24	31.10	0.99	1.11	0.99	29.99	28.8	0.99	2.17	2.30	32.56	32.30	0.99
12	2.29	0.68	17.22	16.50	0.99	2.20	0.51	15.19	14.80	0.99	5.08	1.42	16.71	16.40	0.99

system are given in Tables 1–3. The intercept of the straight line plots of $\log(q_e - q)$ versus t should equal to $\log(q_e)$ and the intercept did not equal to q_e (Table 1) then the reaction is not likely to be first-order, irrespective of the magnitude of the correlation coefficient. The predicted and experimental q_e values for the basic dye–adsorbent system were compared with the three kinetic models (Tables 1–3). Since most of the pseudo-first-order and intraparticle diffusion model values deviate from the experimental values, it suggests that the adsorption of the dye onto the adsorbents follows the pseudo-second-order model. The agreement between the experimental and predicted curves is extremely good. Hence, the concentration of the basic dye in the solution had a strong influence on the pseudo-second-order kinetics. This model also assumes the rate limiting step may be the adsorption in agreement with chemical adsorption being the rate controlling step, which may involve valence forces through sharing or exchange of electrons between dye and adsorbent.

Table 3
The effect of process variables on intraparticle diffusion model constants

Adsorbent	Parameter, C_0 (mg/L)	Model constants			
		k_{id}	$q_{e(mod)}$	$q_{e(exp)}$	r^2
Sepiolite	100	0.273	11.38	16.70	0.95
	200	0.638	16.73	31.10	0.99
	300	0.901	26.55	44.50	0.97
Fly ash	100	0.415	5.55	14.90	0.99
	200	0.854	11.12	28.80	0.98
	300	1.293	14.10	40.30	0.97
ASAC	100	0.259	10.65	16.20	0.96
	200	0.571	19.97	32.30	0.99
	300	0.928	30.98	50.10	0.97
Adsorbent	Parameter, m_s (g/L)	Model constants			
		k_{id}	$q_{e(mod)}$	$q_{e(exp)}$	r^2
Sepiolite	3	0.741	49.52	65.10	0.98
	6	0.638	16.73	31.10	0.99
	12	0.382	8.80	16.50	0.97
Fly ash	3	0.744	39.43	55.10	0.98
	6	0.854	11.12	28.80	0.98
	12	0.288	8.17	14.80	0.99
ASAC	3	1.232	32.25	57.30	0.98
	6	0.571	19.97	32.30	0.99
	12	0.226	11.85	16.40	0.97

It was observed that there were two linear portions (plots not depicted here), indicating two-stage diffusion of dye onto adsorbent materials. The slope of the second linear portion characterizes the rate parameter corresponding to the intraparticle diffusion, whereas the intercept of this second linear portion is proportional to the boundary layer thickness. Table 3 gives the values of k_{id} and model constants for the three adsorbents with respect to initial concentration and adsorbent dose. The values of the initial adsorption rates, h determined from the straight line plots for each adsorbent system, increased with an increase in the initial dye concentration can be attributed to the increase in the driving force for mass transfer, allowing more dye molecules to reach the surface of the adsorbents in a shorter period of time.

The corresponding linear plots of the values of q_e, k_2 and h versus C_0 were regressed to obtain expressions for these values in terms of the initial dye concentration with high correlation

Table 4
Empirical parameters for predicted q_e, k_2, and h

Parameter	Adsorbent	A_{q_e}	B_{q_e}	A_{k_2}	B_{k_2}	A_h	B_h
C_0 (mg/L)	Sepiolite	4.15×10^{-3}	5.36	768.54	−47007.9	0.02×10^{-2}	107.06
	Fly ash	2.34×10^{-3}	6.32	1446.34	−95657.5	-11.45×10^{-2}	229.16
	ASAC	-0.36×10^{-3}	6.12	777.98	−53169.1	-9.99×10^{-2}	105.74
m_s (g/L)	Sepiolite	187.62	−0.97	3.09×10^{-4}	0.788	39.14	−1.66
	Fly ash	157.89	−0.94	2.49×10^{-4}	0.865	25.01	−1.63
	ASAC	160.90	−0.91	2.73×10^{-4}	1.172	7.14	−0.65

coefficients (Table 4). Therefore, it is useful for process design purposes if the terms q_e, k_2 and h can be expressed as a function of C_0 for the dye as follows [24,25]:

$$q_e = \frac{C_0}{A_{q_e} C_0 + B_{q_e}} \quad (6)$$

$$k_2 = \frac{C_0}{A_{k_2} C_0 + B_{k_2}} \quad (7)$$

$$h = \frac{C_0}{A_h C_0 + B_h} \quad (8)$$

Substituting the values of q_e and h from Table 2 into Eqs. (6)–(8) and then Eq. (4) derives the rate law for pseudo-second-order and the relationship of q, C_0 and t for each adsorbent can be presented in the following equations:

$$q = \frac{C_0 t}{(4.15 \times 10^{-3} C_0 + 5.36)t - 1.62 \times 10^{-4} C_0 + 107.06} \quad \text{(for sepiolite)} \quad (9)$$

$$q = \frac{C_0 t}{(2.34 \times 10^{-3} C_0 + 6.32)t - 11.45 \times 10^{-2} C_0 + 229.16} \quad \text{(for fly ash)} \quad (10)$$

$$q = \frac{C_0 t}{(-3.56 \times 10^{-4} C_0 + 6.12)t - 9.99 \times 10^{-2} C_0 + 105.74} \quad \text{(for ASAC)} \quad (11)$$

Eqs. (9)–(11) show generalized predictive models for the amount of the dye adsorbed at any contact time and initial concentration within the given ranges. The equations clearly indicate that the dye adsorbed at any contact time per unit mass is higher for a greater initial dye concentration.

4.2. Effect of adsorbent dose on adsorption kinetics

The effect of the adsorbent dose on the adsorption rate of the basic dye was investigated with adsorbent dose varying from 3 to 12 g/L at fixed pH, temperature and dye concentration. The study shows an enhancement in adsorption with the increase in dose of the adsorbent (Fig. 3). The amount dye adsorbed increases from 16.5 to 65.1 mg/g for sepiolite, from 14.8 to 55.1 mg/g for fly ash and from 16.4 to 57.3 mg/g for ASAC, respectively, when the amount of adsorbent is increased from 3 to 12 g/L.

A plot of t/q against t for adsorption of the basic dye for the pseudo-second-order model and a plot of q against the square

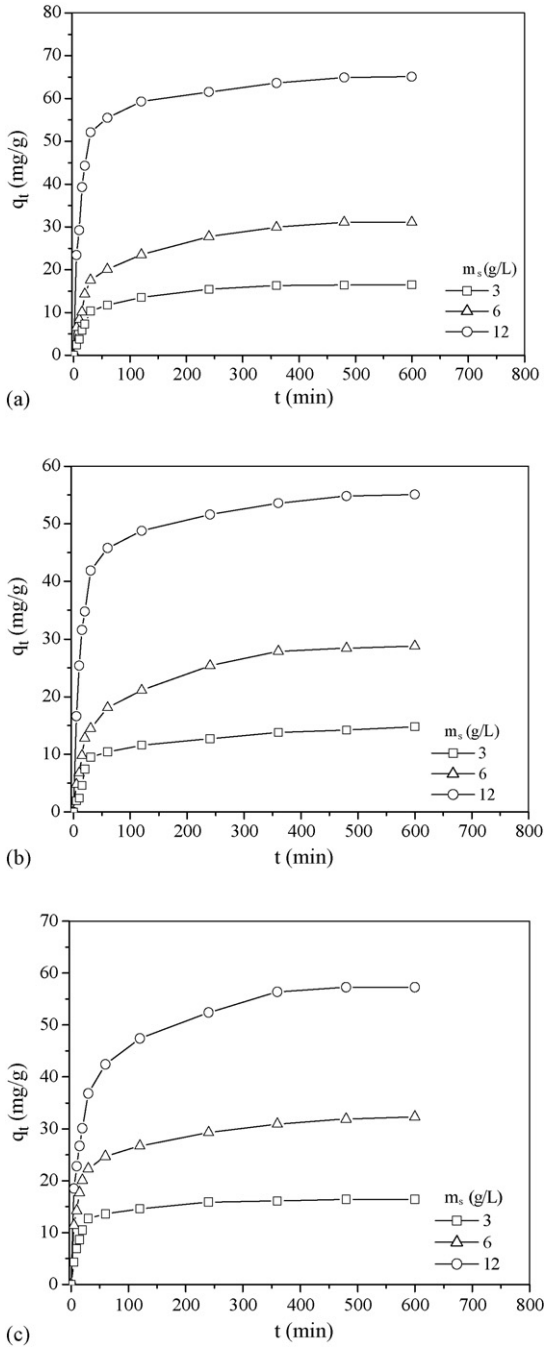

Fig. 3. Effect of adsorbent dose onto (a) sepiolite, (b) fly ash and (c) ASAC. Experimental conditions: C_0 = 200 mg/L; T = 303 K; 250 rpm.

root of t for the intraparticle diffusion rate model onto three adsorbents (plots not depicted) used to calculate values of the rate constants for three kinetic models are shown in Tables 1–3. The data showed good compliance with the pseudo-second-order kinetic model in terms of higher correlation coefficients (>0.99) and very close values of predicted and experimental q_e for the dye–adsorbent system. There was a decrease in h, the initial rate parameter with adsorbent dose (Table 2). The values of k_2 increased with increasing adsorbent dose which result in an increase in the surface area for adsorption and an increase in the available sites for adsorption. The intraparticle diffusion coefficients are all high (>0.95) which suggests that for the dye adsorption onto the adsorbents the mechanism is predominantly intraparticle diffusion but the distinction is not completely clear. The rate controlling mechanism may change during the course of adsorption process. Three possible mechanisms may be occurring. There is an external mass transfer of film diffusion process that controls the early stages of the adsorption process. This may be followed by a constant rate stage and finally by a diffusion stage where the adsorption process slows down considerably. The overall of the dye adsorption process appears to be controlled by the chemical process in this case in accordance with the pseudo-second-order reaction mechanism.

The corresponding linear plots of the values of q_e, k_2 and h versus the adsorbent dose, m_s for the dye were regressed to obtain expressions for these values in terms of m_s with high correlation coefficients (Table 4). Therefore, it is further considered that q_e, k_2 and h can be expressed as a function of m_s as follows [24,25]:

$$q_e = A_{q_e}(m_s)^{B_{q_e}} \quad (12)$$

$$k_2 = A_{k_2}(m_s)^{B_{k_2}} \quad (13)$$

$$h = A_h(m_s)^{B_h} \quad (14)$$

Substituting the values of q_e and h from Table 2 into Eqs. (12)–(14) and then Eq. (4) derives the rate law for pseudo-second-order and the relationship of q, C_0 and t for each adsorbent:

$$q = \frac{t}{[1/(3.09\times10^{-4}m_s^{0.788})(187.62m_s^{-0.967})^2] + [t/187.62m_s^{-0.967}]} \quad \text{(for sepiolite)} \quad (15)$$

$$q = \frac{t}{[1/(2.49\times10^{-4}m_s^{0.865})(157.89m_s^{-0.938})^2] + [t/157.89m_s^{-0.938}]} \quad \text{(for fly ash)} \quad (16)$$

$$q = \frac{t}{[1/(2.73\times10^{-4}m_s^{1.172})(160.90m_s^{-0.906})^2] + [t/160.90m_s^{-0.906}]} \quad \text{(for ASAC)} \quad (17)$$

These equations can be used to derive the amount of dye adsorbed at any given reaction time for any adsorbent dose within the given range. The result also indicates that the dye adsorbed at any contact time is lower for a greater adsorbent dose.

4.3. Adsorption isotherms

The equilibrium adsorption isotherm is of importance in the design of adsorption systems. Several adsorption isotherm equations are available and the two important isotherms are selected in this study, the Langmuir and Freundlich isotherms [26].

The Langmuir model assumes that the uptake of adsorbate occur on a homogeneous surface by monolayer adsorption without any interaction between adsorbed ions. The Langmuir's equation can be expressed in a mathematical form as shown in Eq. (18):

$$\frac{C_e}{q_e} = \frac{1}{Q_0 b} + \frac{C_e}{Q_0} \quad (18)$$

where C_e is the equilibrium concentration (mg/L), q_e the amount adsorbed at equilibrium (mg/g), Q_0 the adsorption capacity (mg/g) and b is the energy of adsorption (Langmuir constant, L/mol). The maximum adsorption capacity and Langmuir constant were calculated from the slope and intercept of the linear plots C_e/q_e versus C_e which gives a straight line of slope $1/Q_0$ which corresponds to complete monolayer coverage (mg/g) and the intercept is $1/Q_0b$ (Fig. 4). The results are presented in Table 5. The Langmuir parameters, Q_0 and b, were found to

Table 5
Isotherm parameters for adsorption of the basic dye by various adsorbents

Adsorbent	Temperature, T (K)	Langmuir isotherm constants			Freundlich isotherm constants			Separation parameter, R_L
		Q_0	b	r^2	k_F	$1/n$	r^2	
Sepiolite	303	155.52	0.0064	0.995	5.294	0.4872	0.986	0.049–0.57
	313	190.11	0.0066	0.997	6.666	0.4850	0.988	0.047–0.56
	323	209.21	0.0099	0.998	11.651	0.4260	0.979	0.032–0.46
Fly ash	303	128.21	0.0057	0.997	4.761	0.4688	0.987	0.054–0.60
	313	141.84	0.0092	0.999	11.165	0.3653	0.985	0.034–0.48
	323	152.44	0.0123	0.999	17.033	0.3178	0.984	0.026–0.41
ASAC	303	181.50	0.0055	0.996	5.952	0.4890	0.987	0.056–0.61
	313	188.68	0.0076	0.999	7.730	0.4685	0.974	0.042–0.53
	323	201.61	0.0083	0.999	9.305	0.4526	0.969	0.038–0.51

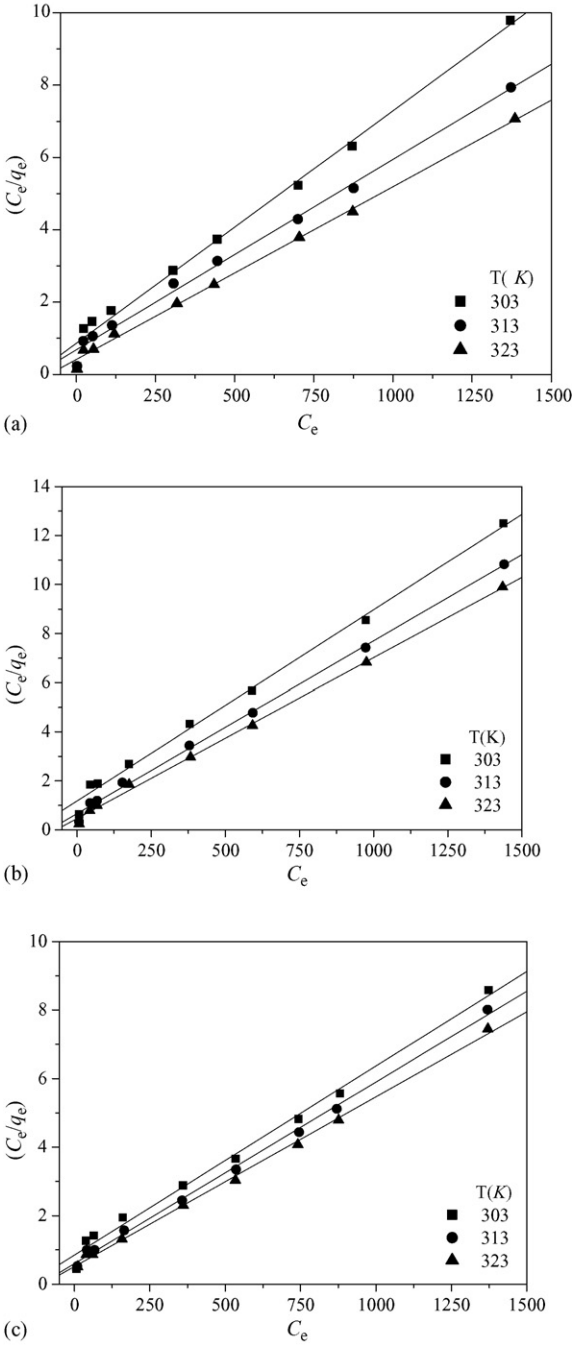

Fig. 4. Langmuir isotherm plots for the adsorption of the basic dye at different temperatures by different adsorbents: (a) sepiolite, (b) fly ash and (c) ASAC.

be increased with temperature. High temperatures increased the kinetic energy of the dye and therefore enhanced the mobility of the dye ions. This led to a higher chance of the dye being adsorbed onto the adsorbent and an increase in its adsorption capacity which results in the enlargement of pore size or activation of the adsorbent surface. This agreed well with the findings in Ref. [27].

The essential feature of the Langmuir isotherm can be expressed by means of dimensionless constant separation factor or equilibrium parameter, R_L, which is calculated using the following equation:

$$R_L = \frac{1}{1 + bC_0} \tag{19}$$

The values of R_L calculated as above equation are incorporated in Table 5.

R_L values lie between 0 and 1 indicates the on-going adsorption process is favorable for the dye using different adsorbents.

The Freundlich isotherm describes equilibrium on heterogeneous surfaces and hence does not assume monolayer capacity.

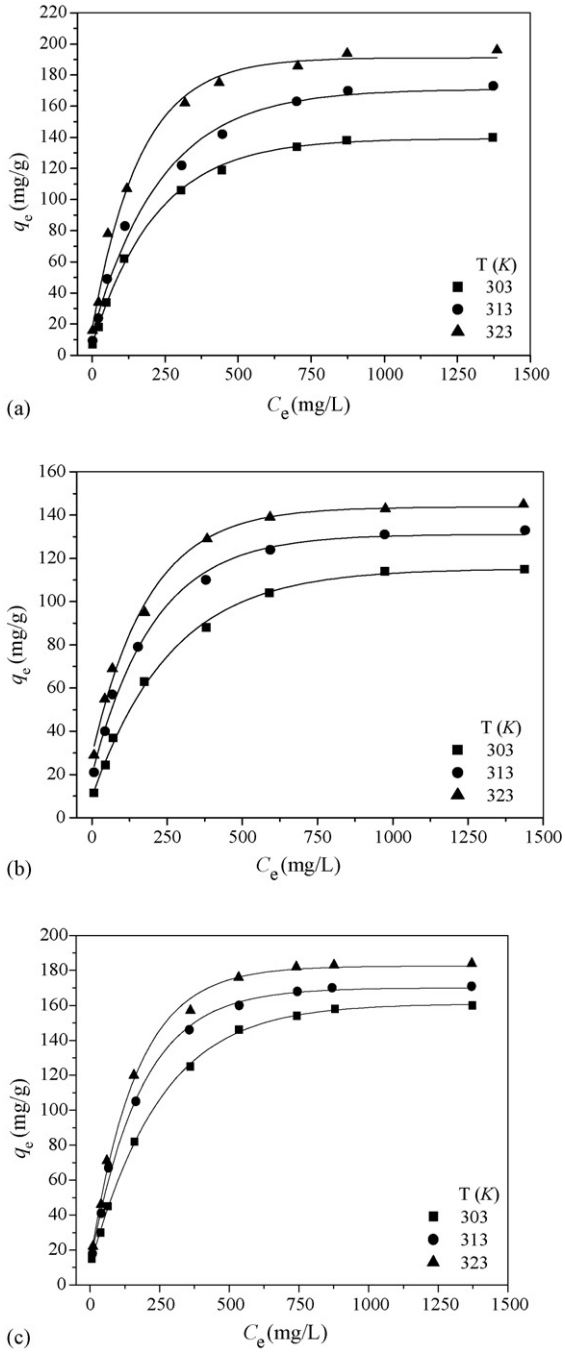

Fig. 5. Effect of temperature on the adsorption of the basic dye onto (a) sepiolite, (b) fly ash and (c) ASAC.

The isotherm is described by the following equations:

$$q_e = k_F C^{1/n} \quad (20)$$

The linearized form of the equation can be written as follows

$$\log(q_e) = \log k_F + \frac{1}{n}\log(C_e) \quad (21)$$

where k_F and n are Freundlich constants and were calculated from the slope and intercept of the Freundlich plots. The Freundlich parameters at different temperatures for the adsorption of the dye onto three adsorbents are shown in Table 5. It has been shown that n values between 1 and 10 represent that the dye was favorably adsorbed onto the adsorbents. The fit of the data for the dye onto these adsorbents suggests that Langmuir model ($r^2 > 0.999$) gave closer fittings than the Freundlich model.

4.4. Effect of temperature

The amount of dye adsorbed at different temperatures (303–323 K) has been examined to obtain thermodynamic parameters for the adsorption system. Adsorption increased with increase in temperature is shown in Fig. 5. The increase in adsorption with a rise in temperature can be explained on the basis of thermodynamic parameters, change in free energy (ΔG°), enthalpy (ΔH°) and entropy (ΔS°) were calculated by using the following equations:

$$\Delta G^\circ = -RT \ln K_c \quad (22)$$

$$\log K_c = \frac{\Delta S^\circ}{2.303R} - \frac{\Delta H^\circ}{2.303R}\left(\frac{1}{T}\right) \quad (23)$$

where K_c, R and T are the equilibrium constant of the adsorption process expressed as the product of the Langmuir constants $b(=K_c)$, gas constant and absolute temperature, respectively.

Table 6
Thermodynamic parameters for adsorption of the basic dye on various adsorbents

Adsorbent	Temperature, T (K)	Thermodynamic parameters		
		$-\Delta G^\circ$ (kJ/mol)	ΔH° (kJ/mol)	ΔS° (kJ/mol K)
Sepiolite	303	12.73	17.82	0.016
	313	13.05		
	323	17.76		
Fly ash	303	13.02	31.31	0.061
	313	12.21		
	323	11.82		
ASAC	303	13.10	16.60	0.012
	313	12.70		
	323	12.87		

ΔH° and ΔS° were calculated from the slope and intercept of van't Hoff plots of $\ln K_c$ versus $1/T$ (plots not shown). The results are given in Table 6. The values of ΔH° varied in the range of 16.60–31.31 kJ/mol indicated that the process is endothermic. The variations in ΔH° values confirm the formation of strong chemical bonds between the dye molecules and the adsorbents and adsorption process was likely to be chemisorption, probably indicating adsorbent/dye complexation. ΔG° values were negative and varied from 11.82 to 17.76 in the temperature range of 303–323 K indicating that the adsorption process led to a decrease in Gibbs free energy. Negative ΔG° indicates the feasibility and spontaneity of the adsorption process. The positive values of ΔS° suggest that the increased randomness at the solid–solution interface during the adsorption of the dye in aqueous solution on the adsorbents. The adsorbed solvent molecules which are displaced by the adsorbate species gain more translational entropy than is ions lost by adsorbate thus allowing

Table 7
Maximum adsorption capacity of various basic dyes by some adsorbents

Adsorbent	Adsorbate	Q_0 (mg/g)	Reference
Clay	Basic Red 9, Basic Violet 3, Basic Violet 4	345, 70, 51	[28]
Palm fruit bunch particle	Basic Yellow	327	[38]
Palm kernel shell activated carbon	Basic Blue 9	311	[29]
Peat, Kudzu	Astrazon Yellow 7GL	300, 270	[31,32]
Activated carbon	Basic Violet 10, Basic Violet 3, Basic Red 9	254, 244, 127	[33]
Peat, Kudzu	Maxilon Red BL-N	240, 219	[31,32]
Sepiolite	Astrazon Blue FGRL	209	This study
Coir pith	Basic Violet 10	203	[37]
ASAC	Astrazon Blue FGRL	202	This study
Activated carbon (F-400)	Basic Blue 69	202	[30]
Diatomaceous earth	Methylene Blue	198	[36]
Palm fruit bunch particle	Basic Red, Basic Blue	180, 91	[38]
Activated carbon	Maxilon Schwarz FBL-01	159	[34]
Bagasse pith	Basic Blue 69, Basic Red 22	158, 77	[36]
Fly ash	Astrazon Blue FGRL	152	This study
Zeolite	Maxilon Goldgelb GL EC	56	[34]
Macroalga *C. lentillifera*	Astrazon Blue FGRL	49	[9]
Activated carbon	Basic Fuchsin	34	[4]
Bagasse pith	Basic Red 22, Basic Blue 69	18, 16	[34]
Activated carbon	Maxilon Schwarz FBL-01	15	[34]
Silica	Basic Blue 3	11	[35]

for prevalence of randomness in the system. The parameters, ΔH°, ΔS°, and ΔG°, for the adsorbate–adsorbent interactions changed in a way that made the adsorption thermodynamically feasible with a high degree of affinity of the dye molecules for the adsorbent surface.

4.5. Comparison of adsorbents

A comparative evaluation of the adsorbent capacities of various types of adsorbents for the adsorption of basic dyes is listed in Table 7. The adsorption capacities of the adsorbents used in this study were not among the highest available but a relatively high uptake capacity of the dye could be obtained which makes the adsorbents suitable for colors removal in textile industry.

5. Conclusions

The adsorption kinetic and equilibrium parameters such as kinetic rate constants, the Langmuir and Freundlich constants, maximum capacity of adsorption, enthalpy of adsorption, were obtained from the adsorption experiments. These parameters are very important for scale-up batch experiments. The removals of the dye by various adsorbents were dependent on the concentration of the dye since the increase in the initial dye concentration increased the amount of the dye adsorbed on the adsorbents. The concentration of the adsorbate on the adsorbent increased with a decrease in the adsorbent dose. A comparison of kinetic models on the overall adsorption rate showed that dye/adsorbent system was best described by the pseudo-second-order rate model. The internal diffusion rate decreased with an increase in mass due to the increased external surface for adsorption. Equations were developed using the pseudo-second-order model that accurately predict the amount of the basic dye adsorbed at any contact time, initial dye concentration and adsorbent dose within the given range. The adsorption data fitted well the Langmuir isotherm. Thermodynamical parameters were also evaluated for the basic dye and revealed that the adsorption of the dye is endothermic in nature. The experimental results showed that these adsorbents could potentially be used in the removal of the basic dyes in aqueous solutions and industrial wastewater treatments.

References

[1] H. Zollinger, Colour Chemistry—Synthesis, Properties and Application of Organic Dyes and Pigments, VCH, New York, 1987.

[2] T. Robinson, G. McMullan, R. Marchant, P. Nigam, Remediation of dyes in textile effluent: a critical review on current treatment technologies with a proposed alternative, Bioresour. Technol. 77 (2001) 247–255.

[3] S.J.T. Pollard, G.D. Fowler, C.J. Sollars, R. Perry, Low-cost adsorbents for waste and wastewater treatment: a review, Sci. Tot. Environ. 116 (1992) 31–52.

[4] V.K. Gupta, I. Ali, Suhas, D. Mohan, Equilibrium uptake and sorption dynamics for the removal of a basic dye (basic red) using low-cost adsorbents, J. Colloid Interf. Sci. 265 (2003) 257–264.

[5] M. Kobya, E. Demirbaş, S. Öncel, S. Şencan, Adsorption kinetic models applied to nickel ions on hazelnut shell activated carbons, Adsorp. Sci. Technol. 20 (2002) 179–188.

[6] M. Kobya, E. Demirbas, E. Senturk, M. Ince, Adsorption of heavy metal ions from aqueous solutions by activated carbon prepared from apricot stone, Bioresour. Technol. 96 (2005) 1518–1521.

[7] S. Wang, L. Li, H.W. Wu, Z.H. Zhu, Unburned carbon as a low cost adsorbent for dye removal, J. Colloid Interf. Sci. 292 (2005) 336–343.

[8] S. Wang, H.T. Li, Dye adsorption on unburned carbon: kinetics and equilibrium, J. Hazard. Mater. 126 (2005) 71–77.

[9] K. Marungrueng, P. Pavasant, Removal of basic dye (Astrazon Blue FGRL) using macroalga *Caulerpa lentillifera*, J. Environ. Manage. 78 (2006) 268–274.

[10] E. Demirbas, M. Kobya, E. Senturk, T. Ozkan, Adsorption kinetics for the removal of chromium(VI) from aqueous solutions on the activated carbons prepared from agricultural wastes, Water SA 30 (2004) 533–539.

[11] K. Kadirvelu, M. Palanival, R. Kalpana, S. Rajeswari, Activated carbon from an agricultural by-product, for the treatment of dyeing industry wastewater, Bioresour. Technol. 74 (2000) 263–265.

[12] M. Alkan, O. Demirbas, S. Celikcapa, M. Dogan, Sorption of Acid Red 57 from aqueous solution onto sepiolite, J. Hazard. Mater. B116 (2004) 135–145.

[13] S. Akyuz, T. Akyuz, A.E. Yakar, FT-IR spectroscopic investigation of adsorption of 3-aminopyridine on sepiolite and montmorillonite from Anatolia, J. Mol. Struct. 565 (2001) 487–491.

[14] K. Brauner, A. Preisinger, Structure and origin of sepiolite, Miner. Petr Mitt. 6 (1956) 120–140.

[15] O. Bayat, Characterisation of Turkish fly ashes, Fuel 77 (1997) 1059–1066.

[16] S. Wang, M. Soudi, L. Li, Z.H. Zhu, Coal ash conversion into effective adsorbents for removal of heavy metals and dyes from wastewater, J. Hazard. Mater. 133 (2006) 243–251.

[17] S. Wang, Y. Boyjoo, A. Chouei, A comparative study of dye removal using fly ash treated by different methods, Chemosphere 60 (2005) 1401–1407.

[18] S. Chakraborty, S. De, S.D. Gupta, J.K. Basu, Adsorption study for the removal of a basic dye: experimental and modeling, Chemosphere 58 (2005) 1079–1086.

[19] Q. Sun, L. Yang, The adsorption of basic dyes from aqueous solution on modified peat–resin particle, Water Res. 37 (2003) 1535–1544.

[20] S.J. Allen, G. McKay, K.Y.H. Khader, Intraparticle diffusion of a basic dye during adsorption onto sphagnum peat, Environ. Pollut. 56 (1989) 39–50.

[21] G. Kahr, F.T. Madsen, Determination of the cation exchange capacity and the surface area of bentonite, illite and kaolinite by methylene blue adsorption, Appl. Clay Sci. 9 (1995) 327–336.

[22] C. Sentorun-Shalaby, M.G. Ucak-Astarlıoglu, L. Artok, C. Sarıcı, Characterization of activated carbons by one-step steam pyrolysis/activation from apricot stones, Micropor. Mesopor. Mater. 88 (2006) 126–134.

[23] W.J. Weber Jr., J.C. Morris, Kinetics of adsorption on carbon from solution, J. Sanit. Eng. Div. Am. Soc. Civ. Eng. 89 (1963) 31–60.

[24] Y.S. Ho, G. McKay, A kinetic study of dye sorption by biosorbent waste product pith, Res. Conserv. Recycl. 25 (1999) 171–193.

[25] S.J. Allen, Q. Gan, R. Matthews, P.A. Johnson, Kinetic modeling of the adsorption of basic dyes by Kudzu, J. Colloid Interf. Sci. 286 (2005) 101–109.

[26] E. Demirbas, Adsorption of cobalt(II) from aqueous solution onto activated carbon prepared from hazelnut shells, Adsorp. Sci. Technol. 21 (2003) 951–963.

[27] K.R. Hall, L.C. Eagleton, A. Acrivos, T. Vermeulen, Pore and solid diffusion kinetics fixed bed adsorption under constant pattern conditions, Ind. Eng. Chem. Res. Fund. 5 (1996) 212–213.

[28] W.T. Tsai, Y.M. Chang, C.W. Lai, C.C. Lo, Adsorption of basic dyes in aqueous solution by clay adsorbent from regenerated bleaching earth, Appl. Clay Sci. 29 (2005) 149–154.

[29] A. Jumasiah, T.G. Chuah, J. Gimbon, T.S.Y. Choong, I. Azni, Adsorption of basic dye onto palm kernel shell activated carbon: sorption equilibrium and kinetics studies, Desalination 186 (2005) 57–64.

[30] D.C.K. Ko, D.H.K. Tsang, J.F. Porter, G. McKay, Applications of multipore model for the mechanism identification during the adsorption of dye on activated carbon and bagasse pith, Langmuir 19 (2003) 722–730.

[31] S.J. Allen, G. Mckay, K.Y.H. Khader, Multi-component sorption isotherms of basic dyes onto peat, Environ. Pollut. 52 (1988) 39–53.

[32] S.J. Allen, Q. Gan, R. Matthews, P.A. Johnson, Comparison of optimised isotherm models for basic dye adsorption by Kuzdu, Biores. Technol. 88 (2003) 143–152.

[33] K.V. Kumar, S. Sivanesan, Isotherm parameters for basic dyes onto activated carbon: comparison of linear and non-linear method, J. Hazard. Mater. B129 (2006) 147–150.
[34] V. Meshko, L. Markovska, M. Mincheva, A.E. Rodrigues, Adsorption of basic dyes on granular activated carbon and natural zeolite, Water Res. 35 (2001) 3357–3366.
[35] M.N. Ahmad, R.N. Ram, Removal of basic dye from waste-water using silica as adsorbent, Environ. Pollut. 77 (1992) 79–86.
[36] M.A. Al-Ghouti, M.A.M. Khraisheh, S.J. Allen, M.N. Ahmad, The removal of dyes from textile wastewater: a study of the physical characteristics and adsorption mechanisms of diatomaceous earth, J. Environ. Manage. 69 (2003) 229–238.
[37] C. Namasivayam, M.D. Kumar, K. Selvi, R.A. Begum, T. Vanathi, R.T. Yamuna, Waste' coir pith—a potential biomass for the treatment of dyeing wastewaters, Biomass Bioenergy 21 (2001) 477–483.
[38] M.M. Nassar, Y.H. Magdy, Removal of different basic dyes from aqueous solutions by adsorption on palm-fruit bunch particle, Chem. Eng. J. 66 (1997) 223–226.